Photoswitchable Water-Soluble Quantum Dots: pcFRET Based on Amphiphilic Photochromic Polymer Coating

Sebastián A. Díaz,[†] Guillermo O. Menéndez,[†] María H. Etchehon,[†] Luciana Giordano,[‡] Thomas M. Jovin,[‡] and Elizabeth A. Jares-Erijman[†,*]

[†]Departamento de Química Orgánica, Facultad de Ciencias Exactas y Naturales, Universidad de Buenos Aires, CIHIDECAR, CONICET, 1428 Buenos Aires, Argentina, and [‡]Laboratory of Cellular Dynamics, Max Planck Institute for Biophysical Chemistry, Am Fassberg 11, 37077 Göttingen, Germany

ABSTRACT A novel surface architecture was developed to generate biocompatible and stable photoswitchable quantum dots (psQDs). Photochromic diheteroarylethenes, which undergo thermally stable photoconversions between two forms with different spectral properties in organic solvents, were covalently linked to an amphiphilic polymer that self-assembles with the lipophilic chains surrounding commercial hydrophobic core−shell CdSe/ZnS QDs. This strategy creates a small (~7 nm diameter) nanoparticle (NP) that is soluble in aqueous medium. The NP retains and even enhances the desirable properties of the original QD (broad excitation, narrow emission, photostability), but the brightness of its emission can be tailored by light. The modulation of emission monitored by steady-state and time-resolved fluorescence was 35−40%. The psQDs exhibit unprecedented photostability and fatigue resistance over at least 16 cycles of photoconversion.

KEYWORDS: FRET · quantum dots · photochromism · amphiphilic polymer · nanoparticle coating

Of the fluorescent probes currently available for biological imaging, many exploit the unique properties of inorganic quantum dots (QDs): broad excitation, narrow emission, photostability, and brightness. QDs are replacing traditional organic fluorophores in many areas, including multiplexed analysis, cell sorting and tracking, and cellular and molecular imaging.[1] QDs function as Förster resonance energy transfer (FRET) donors and acceptors.[2−5] If certain spectroscopic criteria are met, the energy from an excited donor QD can be transferred to one or more proximal ground-state acceptors. Photochromic (PC) compounds are characterized by a reversible transformation that occurs when they are illuminated cyclically at appropriate wavelengths. The transition is between two different structural forms with distinct absorption spectra. If one of these overlaps the emission of a nearby fluorophore functioning as a donor, the system exhibits switchable FRET, a process we have denoted previously as pcFRET.[6,7] The fluorescence emission of the QD donor can be modulated reversibly by manipulating the state of the PC acceptor with cycles of UV−visible irradiation, allowing greatly increased signal detection by rejection of background signals. For example, phase-sensitive lock-in detection technology has pushed the limit of FRET transfer efficiency to significantly below 1%, greatly enhancing sensitivity in monitoring molecular interactions.[8,9] Immediate applications come to mind for such probes in both cellular tracking, *e.g.*, FRAP[10] and FLIM,[11] and in super-resolution fluorescence localization microscopy, in which controllable and stable transition between bright and dark states is the elemental requirement for sub-diffraction detection.[12−15] Very high on−off contrast is not necessarily required.[16]

pcFRET has been demonstrated previously with QDs[17−19] as well as with organic donors.[6,9,20] Based on this phenomenon, various innovative nanostructures have been proposed, including polymers and SiO_2 nanoparticles (NPs) as scaffolds,[21,22] thereby broadening the fields of application. Yet a major challenge has impeded further progress: the greatly reduced efficiency and stability of photochemical cycling of photochromic compounds in aqueous media, compared to organic solvents. For example, thiophene-based diheteroarylethenes operate very well in organic solvents, showing no spontaneous thermal reversion and undergoing numerous photocycles without fatigue.[23] However, they do not function in water. Recently developed diarylethenes[24] and oxazines[25] incorporate extended amphiphilic side

* Address correspondence to eli@qo.fcen.uba.ar.

Received for review November 29, 2010 and accepted March 4, 2011.

Published online March 04, 2011
10.1021/nn103243c

chains to provide water solubility. They exhibit efficient photoconversion but have yet to be applied in/with NPs acting as FRET donors. Other photoswitchable water-soluble NPs[26] are based on amphiphilic polymers forming self-assembled micelles, including some with multicolor properties.[27] Such NPs are limited by their comparatively large and heterogeneous size (~50−100 nm) and finite stability. In the field of biocompatible dyes the development of various photoswitchable fluorescent proteins has represented a tremendous boon to cellular biologists.[28] Nonetheless the brightness and photostability of fluorescent proteins remains inferior to those of QDs.[29]

Despite their many virtues, colloidal QDs are synthesized in organic solvents and require surface modifications in order to provide solubility in aqueous media and biocompatibility.[30] These aims are achieved either by replacing or by capping the original hydrophobic surface ligands.[31] Capping strategies necessarily lead to larger NPs, yet the stability and quantum yield of the QD are preserved or even improved in comparison to what can be achieved with ligand exchange techniques.[32]

Ligand capping strategies require an amphiphilic polymer that can interact with the original hydrophobic surface ligands and present a hydrophilic surface once it is assembled about the QD. In this study we demonstrate that embedding a photochromic acceptor in such an amphiphilic polymer creates a hydrophilic and stable photoswitchable QD. To this end, we employed the technology introduced by the Parak group for coating QDs with a functionalized core−shell structure.[33] This architecture permits the exploitation of the hydrophobic microenvironment between the surface of the semiconductor QD and the external surface of the assembled NP. We placed the FRET acceptors in this compartment, thereby achieving two ends: providing a chemical environment conducive to efficient and stable photoswitching and maintaining close proximity to the QD donor. This structural design, to our knowledge reported here for the first time, provides an effective pcFRET probe in a small (~7 nm diameter) water-soluble package. Fatigue, due to the thermal conversion of the acceptor and/or photobleaching of the donor, is minimized while retaining the superior properties of the original QD. Polymer-coated QDs are also competent for cellular uptake.[34]

In the following, we refer to the entire NP—comprising the metallic QD core, the organic ligands attached to the QD, and the amphiphilic PC polymer coating—as a *photoswitchable QD* (psQD).

RESULTS AND DISCUSSION

Synthesis of Amphiphilic Photochromic Polymer. The PC diheteroarylethene PC-3 (a diheteroarylperfluorocyclopentene with an amine substitution) was synthesized according to the procedure described in Methods (Scheme 1A) and reacted with polyisobutylene-alt-maleic anhydride (PMA; Sigma-531278, M_w ~6000), followed by addition of dodecylamine, thereby leading to a comb polymer structure with pendant dodecyl and photochromic groups (Scheme 1B). Although PC polymers[35−37] and functionalized amphiphilic polymers[38,39] have been reported previously, to our knowledge a photochromic PMA-based amphiphilic polymer has not.

The synthesis of the asymmetric diheteroarylethene was based on the original procedures developed by Irie *et al.*[23] and Giordano *et al.*[40] A variation of the symmetric diheteroarylperfluorocyclopentene with an amine substitution on the aromatic ring was devised, and a number of modifications were introduced to the previously reported method for preparation of the amphiphilic polymer (see Methods). The adopted nomenclature follows that proposed by the Parak group,[38] according to which modifications to the PMA backbone are represented as percentages of anhydride rings coupled with the added molecules. Thus, a polymer in which 1% of the anhydride rings are modified with the PC group and 75% with dodecylamine chains would be identified as PMA 1PC 75C12. The PC properties of the polymers were confirmed in both organic and aqueous solvents (see Scheme 1C). The polymers were soluble in organic solvents and formed self-assembled micelles in aqueous buffers, leading to a scattering background in the absorption spectra. Concentrated solutions in the open form had a light yellow color; upon photochromic cyclization, induced by exposure to UV irradiation, the color changed to dark violet.

Preparation of Quantum Dots Coated with Photochromic Polymer. The majority of experiments were performed with small (~4.1 nm core diameter, manufacturer's specifications) commercial organic QDs, CdSe/ZnS core−shell nanocrystals with octadecylamine ligands (CZ520, NN-Labs, Fayetteville, AR) and with an emission centered at 547 nm. These were coated ("wrapped") with the photochromic polymer, thereby transferring the hydrophobic QDs to an aqueous medium. The use of other QDs will be specifically noted.

The coating procedure for all QDs (Scheme 2) followed that reported previously.[33] The polymer self-assembly is directed by interdigitations of the lipophilic chains with the aliphatic chains of the QD and orientation of the carboxylic groups to the external aqueous medium.[33] The negative surface charge confers a hydrophilic nature to the assembled psQD, rendering it water-soluble. We have taken advantage of the lipophilic nature of the internal self-assembled polymer-aliphatic chain layer by introducing the photochromic units into this region. This strategy secures two fundamental advantages: (i) confinement of the PC group to a medium similar to that of aliphatic hydrocarbons, optimal for photochromic switching with good efficiency and fatigue resistance; and (ii)

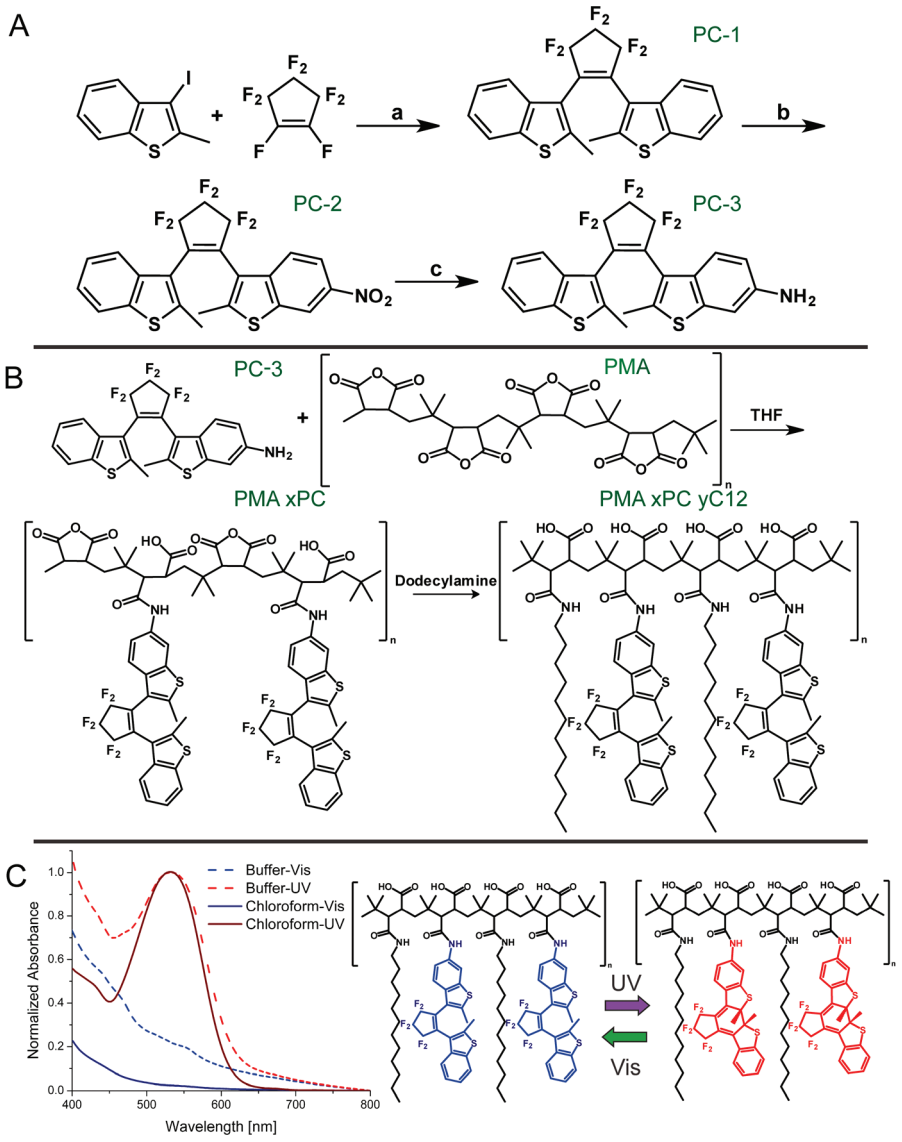

Scheme 1. (A) Synthesis scheme for PC-3: (a) (i) n-BuLi, THF, −78 °C, (ii) C_5F_8; (b) glacial CH_3COOH, $(CH_3CO)_2O$, fuming HNO_3; (c) (i) $NiCl_2 \cdot 6H_2O$, MeOH; (ii) $NaBH_4$. (B) Synthesis scheme for amphiphilic photochromic polymer. (C) Photoconversion of polymer in chloroform and in sodium borate buffer. The spectra were normalized by the visible peaks of the respective photostationary forms.

placement of the PC groups in a restricted zone, at a short distance to the QD surface.

The psQDs were purified and concentrated by two stages of filtration and size exclusion chromatography (Methods). In aqueous media, excess polymer forms empty micelles with a minimum diameter of 30 nm according to determinations by dynamic light scattering (DLS) and electron microscopy (EM), facilitating the separation of excess polymer from the psQDs (diameters of 5−10 nm). The purification of the psQDs was essential for the correct measurement of the pcFRET effect described in the following sections. To determine the influence of empty micelles on the psQDs, three samples were prepared from QDs (NN-Labs CZ540, CdSe/ZnS) emitting at 562 nm and a PMA 0.7PC 55C12 polymer. The preparations were of approximately the same concentration but had different contents of empty micelles: (i) none, being purified as stated, (ii) low, and (iii) high (purification step omitted). Increasing micelle content led to greater scattering, discernible by apparent absorbance in the 600−650 nm range. The reduction in fluorescence after exposure to UV light increased with micellar content (10%, 12%, and 26%, respectively). The quenching in sample (i), attributable exclusively to pcFRET, was 9.5 ± 1.0% according to fluorescence lifetime determinations, in agreement with the steady-state emission of the purified sample.

psQD Characterization and Measurements. Purified samples of psQDs coated with amphiphilic polymer carrying varying amounts of PC moieties were stable for various months upon storage at 4 °C and at alkaline pH

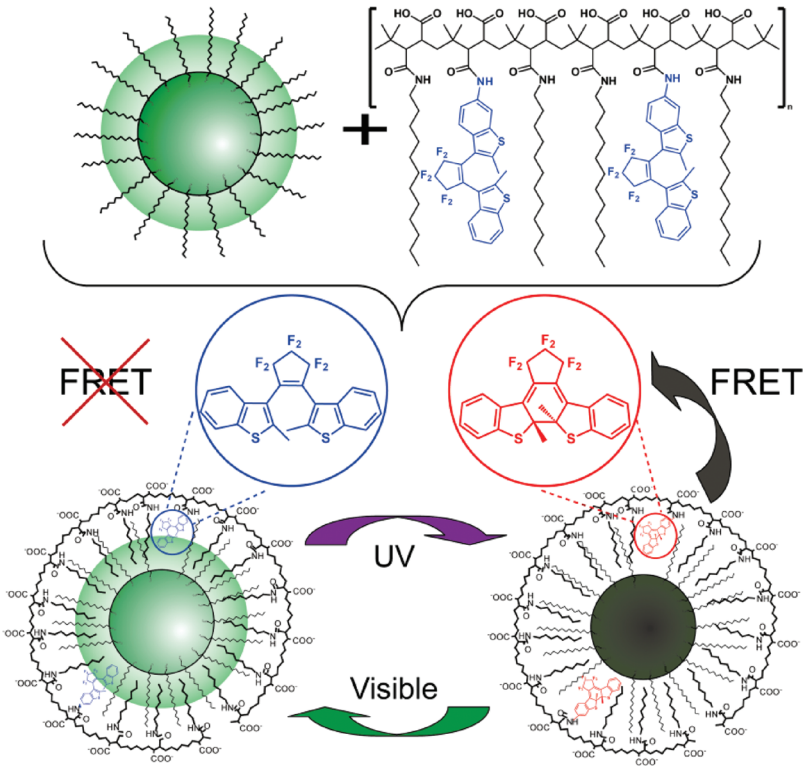

Scheme 2. Photoswitching QDs coated with an amphiphilic photochromic polymer. The fluorescence of the psQD is toggled with FRET by modulating the absorbance of the photochromic polymer with UV and visible light.

(9−12), and for days at room temperature. For short periods of time (hours), for example the time necessary to perform EDC coupling, the preparations could be transferred to pH ≈ 6.5−7. At lower pH (~6) aggregation was observed but was reversed upon alkalinization of the medium. The lipophilic layer of the psQDs and the interior of the micelles reproduce the conditions of the polymer in organic solvents. Therefore extinction coefficients and conversion rates for the PC polymer were estimated using an equivalent PC molecule in organic solvents and making quantitative determinations by absorption and NMR spectroscopy.[6] Applying these values to the PC polymer and the psQDs we estimated the number of PC groups per polymer backbone as well as per psQD. Polymers were prepared with percentages of PC ranging from 0 to 6%.

The rates and extents of photoconversion to the closed and open PC states were monitored by both UV/vis absorption and fluorescence after successive 10 s irradiations with UV (340 ± 10 nm) and visible (545 ± 10 nm) light, respectively (Figure 1 for PMA 6PC 70C12). The course of absorption was fit well by a monoexponential function (with rate constant k_{eq}), as reported previously for this class of PC molecules,[6] although the formalism adopted for the present system leads to an intrinsically more complex behavior (see below). The photoconversion rate constants in the two reaction directions, normalized by the respective irradiances, did not differ significantly. This finding was in accordance with theory, which also states that the rates should increase in the presence of FRET, as was observed in the comparison of the micellar and QD-coated forms (Table 1).

Under the conditions of UV irradiation, the photostationary state at room temperature of the PC polymer was achieved with 22% conversion to the closed state of the PC acceptor (according to NMR analysis, see SI). In view of the 2/3 fraction of open form PC in the photocyclization-competent antiparallel configuration (see SI), the "true" photostationary state under the conditions of experiment would correspond to 33% closed form PC. We assumed, as others have done,[21] an invariant efficiency of photoconversion (albeit in the absence of FRET, see below) in the polymer and polymer−QD associated states.

In the photostationary state established by exposure to 340 ± 10 nm light, the maximal quenching of psQD fluorescence for the sample of Figure 1 was 38% (Figure 2A). The corresponding data for a 2% PC sample are also featured. A quenching of 3 ± 1.5% was exhibited by QDs lacking the PC polymer (Figure 2B); this value was subtracted from the quenching data in Figure 2A. We tentatively attribute this phenomenon to spectral shifts resulting from photooxidation of the QD core induced by UV light[41] in a "susceptible" subpopulation with incomplete passivation shells. Exposure to visible light led to a slight increase in emission, an effect for which numerous photoactivation mechanisms have been proposed.[42] The 6% PC psQD sample was exposed to longer

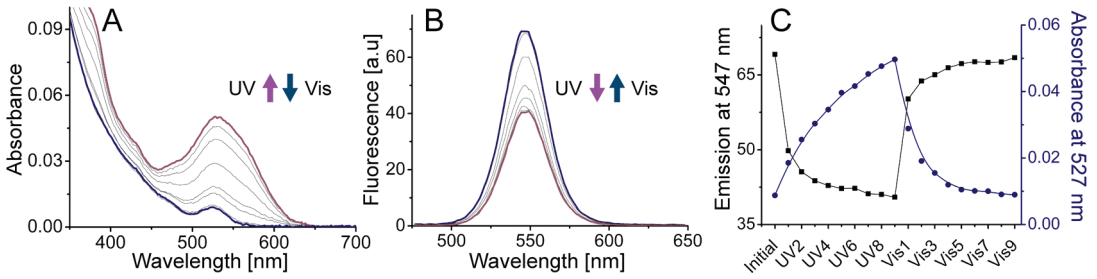

Figure 1. Spectroscopic monitoring of psQDs coated with PMA 6PC 70C12. Irradiation was with sequential 10 s pulses at 340 ± 10 nm (UV, irradiance 1.0 mW/cm^2) and 545 ± 10 nm (vis, irradiance 5.8 mW/cm^2). psQD concentration: 0.2 μM. Temperature: 20 °C. (A) Absorbance spectra of the sample undergoing photoconversion from its initial/open state (blue) to a photostationary state (purple) with UV and then returning to the open state with visible irradiation. (B) Fluorescence spectra corresponding to A. Excitation: 400 nm. (C) Absorbance (blue solid circle) at 527 nm after each irradiation step from A. Fluorescence (black solid square) at 547 nm of each irradiation step from B.

TABLE 1. Photokinetic Parameters of Photochromic Polymer[a]

polymer	$k_{eq}/I_{340\ nm}$, s^{-1} mW^{-1} cm^2	$k_{eq}/I_{545\ nm}$, s^{-1} mW^{-1} cm^2
PMA 2PC 70C12		
micelle	0.009_1	0.008_2
coated on QD	0.013_6	0.010_3
PMA 6PC 70C12		
micelle	0.013_6	0.008_7
coated on QD	0.015_5	0.010_3

[a] I = irradiance: 340 nm, 1.1 mW cm^{-2}; 545 nm, 6.0 mW cm^{-2}. psQDs purified to eliminate micelles. Solutions in 50 mM SBB, pH 9.

periods of irradiation and cycled between the two steady states (Figure 3). The system was stable and demonstrated no fatigue through 16 cycles with a mean quenching of 34 ± 2%.

The relative fluorescence quenching during the initial phases of UV exposure was greater than the corresponding increase in absorbance. We attribute this phenomenon to the inherent dependence of FRET on the number of acceptors and an apparent degree of heterogeneity in the FRET "competency" of the acceptor population, modeled in terms of two distinct classes discussed below.

To confirm that quenching was attributable to FRET, fluorescence lifetime measurements[43] were performed on the psQDs under various conditions (Figure 4). The decays were complex, even with the original QDs, and at least three exponential components were required to adequately, albeit not exactly, represent the time course of deactivation (Methods). The mean lifetimes corresponded well with the values of steady-state fluorescence. The sample presented in Figure 4 had a mean lifetime $\langle\tau\rangle$ of 9.6 ± 0.6 ns for the open state (maximum fluorescence) and of 7.0 ± 0.4 ns for the closed state (minimum fluorescence), corresponding to 27 ± 8% quenching, in good agreement with the ~34% obtained from the steady-state determinations. Most samples demonstrated a somewhat smaller effect in time-resolved than in steady-state fluorescence, a discrepancy that from quantitative estimations is not attributable to trivial reabsorption of the QD emission by the shell of PC groups[44] but rather to the finite absorbance of the closed PC form at the excitation wavelength generally employed (400 nm; extinction coefficients of the open and closed PC states 90 and 5750 M^{-1} cm^{-1}, respectively). The changes in lifetimes were also consistent with those of the calculated emission quantum yields (Table 2; $\partial\tau/\partial QY = 150 \pm 30$ ns).

FRET Formalism. In modeling the system of a QD donor and a shell of a variable number of acceptors, we invoke some of the considerations raised previously with respect to QD-based FRET[43] and the following formalism. We assume a number i of photoconverted (closed) PC groups per QD. The energy transfer efficiency E_i in a psQD with i equivalent acceptors and the corresponding percentage quenching q_i are given by

$$E_i = \frac{i\gamma}{1+i\gamma}; \quad \gamma = \left(\frac{R_o}{r_{DA}}\right)^6; \quad q_i = 100E_i \qquad (1)$$

where r_{DA} is the individual donor−acceptor (QD−PC group) separation and R_o is the Förster transfer distance.[2,7] The quenching data of Figure 2A did not exhibit the asymptotic behavior at high i predicted by eq 1. Thus, we introduce in the analysis an element of complexity in the form of two classes of closed photochromic acceptors linked to the single QD donor. A two-component model is the simplest representation of a heterogeneous population, with the fewest number of additional parameters. The two classes are distinguishable in number and in their FRET efficiency (class 1, by definition, being more efficient), leading to the following expression for the composite FRET efficiency as a function of the relative numbers, i and j, of closed PCs in each class, and their respective transfer efficiency parameters, γ_1 and γ_2.

$$E_{i,j} = \frac{i\gamma_1 + j\gamma_2}{1 + i\gamma_1 + j\gamma_2}; \quad q_{i,j} = 100E_{i,j};$$
$$\gamma_1 = \left(\frac{R_{o,1}}{r_{DA,1}}\right)^6; \quad \gamma_2 = \left(\frac{R_{o,2}}{r_{DA,2}}\right)^6 \qquad (2)$$

The time-dependent fractional photoconversion to the FRET-competent closed form, $\alpha[t]$, is different for

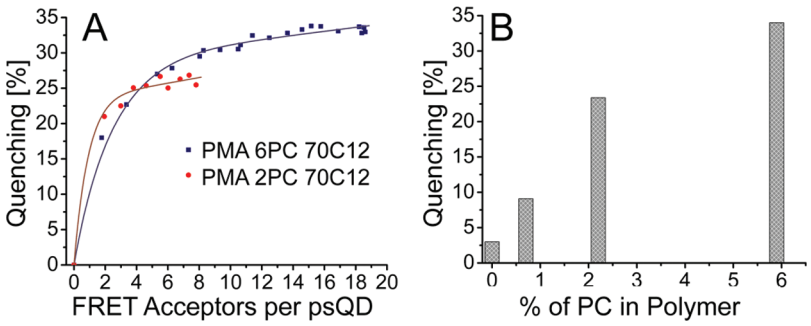

Figure 2. Relation between PC content of a psQD and fluorescence quenching. (A) psQDs with different polymer coatings irradiated with 340 ± 10 nm (1.0 mW cm^{-2}); each dot represents 10 s of irradiation. The FRET acceptors are photocyclized PC moieties. Both sets of data are shown with corresponding fits (see interpretation section). (B) Mean quenching obtained in a number of photocycles (see Figure 3A) of QDs (NN-Labs CdSe/ZnS, 4.1 nm diameter) coated with polymers containing different percentages of PC. The continuous lines in A represent the results of data analyses described below and in the SI. The corresponding individual fits to the time-dependent quenching and PC formation (absorbance) data are shown in Figure S4.

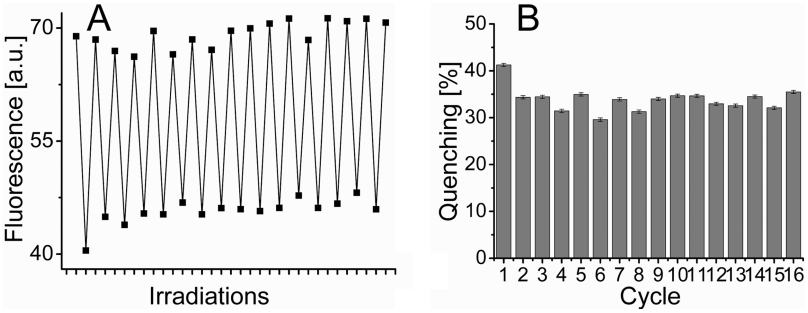

Figure 3. Fluorescence monitoring of psQDs coated with PMA 6PC 70C12 and cycled through on−off states. Irradiation pulses of 60 s with 340 ± 10 nm (1.0 mW cm^{-2}) or 545 ± 10 nm (5.8 mW cm^{-2}) light. psQD concentration: 0.2 μM. Temperature: 20 °C (A) Fluorescence at 547 nm of a sample undergoing photocycling; excitation: 400 nm. (B) Quenching of emission at 547 nm during each cycle observed in A.

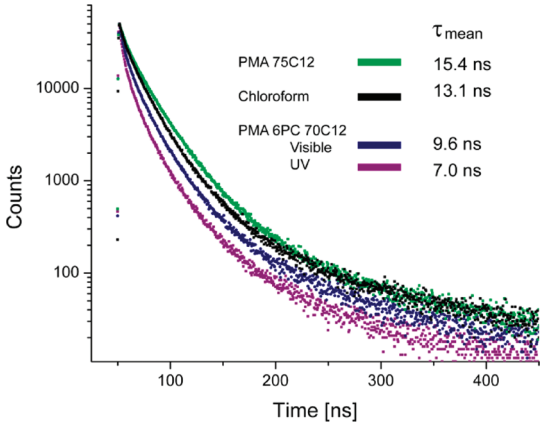

Figure 4. Fluorescence-detected excited-state decays of NN-Labs CZ520, CdSe/ZnS QDs in chloroform, coated with PMA 75C12, or coated with PMA 6PC 70C12 and cycled through the open (visible irradiation)−closed (UV irradiation) states. Emission counts determined at 547 nm.

each class due to the different FRET efficiencies. A higher FRET efficiency results in a higher probability of deactivating an excited QD by energy transfer to one of the closed form members of each class. This, in turn, potentiates the cycloreversion and thus depopulates the closed state and, at the same time, increases the rate, k_{eq}, of the overall reaction. The corresponding differential equations are given by

$$\alpha_{1,2}'[t] = k_{oc}Q_{oc}(1-\alpha_{1,2}[t]) - \left(k_{co}\alpha_{1,2}[t] + k_{QD}\frac{E_{1,2}[t]}{n_{1,2}}\right)Q_{co}$$

$$\frac{E_{1,2}[t]}{n_{1,2}} = \frac{\alpha_{1,2}[t]\gamma_{1,2}}{1+\alpha_1[t]\gamma_1+\alpha_2[t]\gamma_2};$$

$$i[t] = n_1\alpha_1[t]; j[t] = n_2\alpha_2[t] \quad (3)$$

where the rate constants for the forward (open → closed) and reverse (closed → open) photoreactions, k_{oc} and k_{co}, respectively, and for QD excitation, k_{QD}, are given by the product of the respective absorption cross sections and the irradiances.[6] Q_{oc} and Q_{co} are the corresponding quantum yields for the conversion.[6] The subscript 1,2 in eq 3 denotes either population 1 or 2. The potential influences of defined distributions of the parameters n_1, n_2, i, and j on the ensemble properties of the psQD population were considered in detail. The effects were second order, and thus this feature was not retained in the model. Analytical solutions of eq 3 (with 10^{2-4} terms!) were also obtained for the photostationary state.

Evaluation of pcFRET Signals. The above formalism was used to fit the progress curves for PC formation and QD quenching as a function of the time of UV irradiation.

TABLE 2. Properties of Organic QDs and psQDs[a]

sample		% of PC in polymer	diameter,[b] nm	ε_{527}, mM^{-1} cm^{-1}	QD quenching, %	QY[c]	$\langle\tau\rangle$, ns
organic QDs in $CHCl_3$			4.1	45[d]	3.0 ± 1.5[e]	0.22	13.1 ± 0.8
QDs coated with PMA 75C12		0.0	5.8 ± 1.6	45		0.24	15.4 ± 1.2
psQDs coated with PMA 6PC 70C12	visible[f]	5.9	6.7 ± 2.6	46.3		0.20	9.6 ± 0.6
	UV[f]	5.9	6.7 ± 2.6	352	34 ± 2		7.0 ± 0.4

[a] The QDs in all cases were CdSe/ZnS nanocrystals with octadecylamine ligands (NN-Labs). The wavelengths of peak emission (547 nm) and fwhm (31 nm) were unaffected by polymer coating and photoswitching. [b] Values supplied by the manufacturer (for core of original QD) or determined by TEM (Methods). [c] Quantum yield of the QD. Rhodamine 6G in ethanol used as standard. [d] Value provided by the manufacturer. [e] See text for discussion. [f] Samples irradiated with visible or UV light until the photostationary state was reached.

The analyses were constrained by fixing the degree of photoconversion (~22%) in the photostationary state as well as the relation (2:1) between the antiparallel (photoconversion competent) and parallel (photoconversion noncompetent) isomers of the open PC form (see SI).

A global fit was carried out with the combined data of psQDs generated with 2PC and 6PC polymers differing in PC content (2.2% and 5.9%, respectively) by creating a composite difference function and applying the FindMinimum routine of Mathematica (Wolfram Research) to eqs 2 and 3 with a minimum least-squares criterion. Very good fits to the data were achieved (Table 3, Figure S4), and parameter convergence, although dependent on the selection of starting values, was consistent between the various experiments. The polymer preparations with different PC content had kinetic properties consistent with the assumption of a common photoconversion−FRET mechanism and set of rate constants (Tables 1 and 3).

An interesting feature of the photoconversion mechanism relates to the kinetics and extent of photocyclization upon exposure to UV light. The rate constant of photoconversion, given by the sum of the forward and reverse rate constants, $k_{\rightarrow}$ and $k_{\leftarrow}$, respectively, actually changes during photoconversion in the one donor−many acceptor system under consideration, because the FRET efficiencies, and thus $k_{\leftarrow}$, vary continuously with i and j during the course of reaction (eq 3). We take note of our assumption that interconversion between the antiparallel and parallel isomers of the open form PC is slow on the time scale of the experiments. If this is not the case, appropriate modifications to the model can and should be made.

There are two distinguishing features of the psQD that emerge from the quantitative analysis of the data in accordance with the two-class model for the closed FRET-competent PC groups. The first is chemical in nature, the indication being that in the case of both the 2% and 6% PC polymers, 37−38% of the groups are in class 1, distinguished by a much higher FRET efficiency. The second, photochemical feature is the pronounced effect of FRET on the rate and extent of photoconversion of the two classes. Upon UV irradiation, class 1 converts to the closed form much faster but achieves a photostationary value of only 2−4%. Nonintuitively, yet for the same reason (very efficient QD−PC FRET), this class accounts for most of the QD quenching. In contrast, class 2 PC converts more slowly (and dominates the PC time course), reaches 33% in the photostationary state, and contributes much less to quenching by FRET. The treatment also overcomes limitations in a previous determination of the photostationary state of the surface-bound diheteroarylethene, which was assumed to be similar to that of the free dye.[21]

For the PMA 6PC 70C12 (5.9% PC) example of Figure 1, the analysis yielded ~18 closed PC groups/psQD in the photostationary state. For psQDs coated with PMA 2PC 70C12 (2.2% PC) the corresponding value was ~10 (6PC/2PC ratio = 1.8; corresponding content ratio = 2.7). Considering that the number of PC groups, the water content of the solvents, and the number of alkyl chains per polymer influence the final quantity of polymer that caps each QD, the apparent discrepancy between 1.8 and 2.7 is not unexpected; in our case 2% appears to be somewhat more efficient than 6%. Taking into account the isomer ratio and the complex influence of FRET on the photostationary state of the two proposed acceptor classes, the calculated total number of photoconversion-competent molecules for the PMA 6PC 70C12 and PMA 2PC 70C12 polymer formulations were ~84 and ~51, respectively (Table 3; ratio = 1.6). From the definition of the rate constants and knowledge of the absorption cross sections (extinction coefficients) and the irradiances, estimates of the reaction quantum yields were obtained: Q_{oc} = 0.07; Q_{co} = 0.07 (from k_2) and 0.10 (from k_3).

The Förster transfer parameter R_o was computed for the open (1.3 nm) and closed (4.0 nm) forms of the PC acceptor from the spectral data, the refractive index n_{pol} = 1.43,[45] corresponding to the polymeric environment of the acceptor, the reference value for $\kappa^2 = 2/3$,[3] and donor QY = 0.22 (Table 2). The two *in situ* acceptor populations could in principle exhibit different values of γ due to orientation ($R^6_{o,1} = 1.5R^6_o\kappa^2_1$; $R^6_{o,2} = 1.5R^6_o\kappa^2_2$) and/or distance ($r_{DA,1}$, $r_{DA,2}$).

The data analysis indicates that photochromic acceptor classes 1 and 2 differ in (1) the number of molecules: total, n_1 and n_2, and photocyclized, i and j; and (2) FRET efficiency ($\gamma_1 > \gamma_2$). The photocyclization

TABLE 3. Analysis of the UV-Induced Photoconversion and QD Quenching Kinetics[a]

polymer	$10^3k_1 = k_{oc}Q_{oc}$	$10^3k_2 = k_{co}Q_{co}$	$10^3k_3 = k_{QD}Q_{co}$	n_1	n_2	n_{tot}	$\gamma_1 = (R_{o,1}/r_{DA,1})^6$	$\gamma_2 = (R_{o,2}/r_{DA,2})^6$	$\alpha_{ps,1}$	$\alpha_{ps,2}$
PMA 2PC 70 C12	4.4	7.6	0.35	20	31	51	0.69	0.0055	0.02	0.33
PMA 6PC 70 C12[b]	5.0	7.2	0.46	31	52	83	0.40	0.0100	0.04	0.33
PMA 6PC 70 C12[c]	4.7	8.0	0.46	31	54	85	0.34	0.0045	0.04	0.33
mean values	4.7 ± 0.2	7.6 ± 0.4	0.42 ± 0.06				0.48 ± 0.19	0.007 ± 0.003		

[a] All k's in s^{-1}. $\alpha_{PS,2}$ set to indicated value (see psQD Characterization and Measurements). [b] UV-induced photoconversion featured in Figure 1c. [c] UV-induced photoconversion featured in Figure 2a.

rate (but not the extent, see below) and FRET efficiency are favored for PC groups either (i) situated closer to the QD surface ($r_{DA,1} < r_{DA,2}$) and thus experiencing a more nonpolar environment than groups located more externally and/or (ii) in an orientation more favorable for energy transfer by virtue of an absorption transition moment positioned more normal than parallel to the QD surface. The latter case would be manifested by a lower value of the FRET orientation factor κ^2 to which R_o^6 is proportional (see discussion below).

Scheme 3 depicts these proposed situations. Class 1 PC groups are embedded in proximal regions of the "comb" with high chain density, whereas class 2 PC molecules are shown in local regions of the polymer deficient in pendant alkyl chains. [Assuming a random distribution, the probability that a PC on a given polymer chain is surrounded by less than two alkyl chains in the polymer sequence would be 50% in the case of the 70C12 formulation.] These locations presumably exhibit a reduced tendency to engage in interactions with the comb, thus forming an insertion "locus" more removed from the surface of the QD core. Further aspects of Scheme 3 are discussed below.

We now attempt a semiquantitative interpretation of Scheme 3 and the corresponding data of Table 3. Assuming saturation of the 4.1 nm QD surface with (tilted) octadecylamine ligands with a packing density of 18.5 Å^2/molecule,[46] the number of aliphatic chains/NP would be ~300. In the case of the 6PC polymer (6% PC, 70% C12), the estimated number of photoconversion-competent PC groups/psQD is 85 (Table S3), corresponding to a total PC content of ~130 taking the open form PC isomer ratio into account. Thus, for this polymer one can estimate a number of ~1500 (130 × 0.7/0.06) polymer-associated C12 chains/psQD, only ~1/5 of which could/would be associated with the 300 octadecylamine ligands. We interpret this result as indicative of the situation depicted in Scheme 3, in which regions of polymer deficient in pendant chains would be forced away from the QD surface into class 2 "loci". In addition, polymers with backbone lengths of ~40 monomers would not be expected to form a homogeneous cap on the QD surface; one must assume the existence of crossover sites, which would necessarily constitute additional PC displacement to the exterior.

We can supplement the above considerations with estimates derived for the distance Δ of the

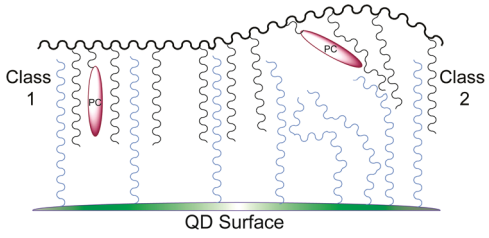

Scheme 3. Heterogeneity of distance and orientation of PC moieties, the FRET acceptors, to the QD surface. The FRET efficiency and photoconversion rate and extent are affected by the PC positioning. In this example, class 2 molecules are shown both further from and oriented less favorably (for FRET) to the QD surface. The pronounced curvature of the QD surface on this size scale and the consequent tilting and splaying of the aliphatic chains are not depicted.

class 1 acceptors from the QD surface using the experimental values of γ_1, the assumption that $R_{o,1} = R_o$, and the relationship[43] $\Delta = R_o\gamma^{-1/6} - r_{QD}(n_{QD}/n_{pol})^{2/3}$. The refractive index term corrects for virtual dilation of intraparticular distances due to propagation in the dense QD semiconductor medium ($n_{QD} = 2.55$).[43] With $r_{QD} = (4.1)/2$ nm, we obtained $\Delta_1 = 1.5$ (range: 1.2−1.9) nm for the high-efficiency FRET acceptors. These values are compatible with the size of the psQD measured by TEM (6.7 nm, Figure S3) and the acceptors being on the inside layer of the polymer shell. A corresponding calculation for acceptor population 2 yields Δ_2 = ~6 nm, an unrealistically large value attributable to the uncertainty in how to interpret the very low value of γ_2. Assuming that the difference in γ_1 and γ_2 is due exclusively to orientation (κ_2^2), such that $\Delta_2 = \Delta_1 = 1.5$, κ_2^2 would be ~0.01, implying a very unfavorable orientation for transfer (Figure 3). More generally, $\kappa_2^2/r_{DA,2} \ll \kappa_1^2/r_{DA,1}$ such that both distance and orientation effects could be involved. For example, for $\Delta_2 = 3.5$ nm, κ_2^2 would be ~0.1. Tables 1−3 summarize all given and derived parameters for the psQD system. From an operational standpoint, the assumption of two classes of acceptors, distinguishable by their FRET properties, accounts very satisfactorily for the observed properties of the psQD system.

CONCLUSION

We have demonstrated the phase transfer of small QDs, photoswitchable by pcFRET, from an organic to an aqueous medium by using an amphiphilic

photochromic polymer as a ligand capping reagent. In so doing, we took advantage of a previously underutilized microenvironment, the hydrophobic region between the QD surface and the hydrophilic exterior of the polymer coat. The psQD retains all the desirable properties of the original QD (broad excitation, narrow emission, photostability) and allows the brightness of the emission to be tailored by something as noninvasive as light. This particular architecture can be exploited to introduce other hydrophobic molecules into a NP system. Table 2 compares the properties of QDs in (i) their original form (in $CHCl_3$), (ii) coated with a PC-free polymer (in water), and (iii) coated with a PC polymer in both the open and closed state. The system can be optimized further by achieving greater overlap between the QD emission and PC absorption as well as by additional PC tailoring allowing for better conversion rates and closer placement to the QD surface. Both effects would enhance FRET and therefore quenching. The photophysical model of the system is quite complex, and future studies will be required to refine it. The hydrophilic nature of the psQD opens up numerous applications in biological and live cell studies, particularly since the external carboxyl groups can be used to further functionalize the nanoparticles.

METHODS

Chemicals. All reagents were obtained from Sigma-Aldrich unless otherwise indicated.

Synthesis of Photochromic Diheteroarylethenes. *PC-1 = 3,3′-(3,3,4,4,5,5-Hexafluorocyclopent-1-ene-1, 2-diyl)bis(2-methylbenzo[b]thiophene).* A solution of *n*-butyllithium (1.6 M in hexane, 2.22 mL) was added to a solution of 3-iodo-2-methylbenzo[*b*]thiophene (1 g) in 15 mL of anhydrous THF at −78 °C under an inert Ar atmosphere. The solution was stirred for one hour, and a white precipitate was observed. At this point 0.25 mL of perfluorocyclopent-1-ene (Zeon Chemicals L.P.) was added. The solution turned yellow and after one hour at −78 °C was allowed to reach room temperature. The solution was neutralized with 30 mL of 1 N HCl. The crude reaction was extracted with ethyl acetate (2 × 20 mL), and the organic phase was washed with brine, dried with Na_2SO_4, filtered, and evaporated in a Rotovap system. Purification was performed on a silica gel column with cyclohexane as solvent, with the final product of 3,3′-(3,3,4,4,5,5-hexafluorocyclopent-1-ene-1,2-diyl)bis(2-methylbenzo[*b*]thiophene) as a white solid (0.48 g, 57%). Characterization was in accordance with reported information.[47]

PC-2 = 3-(3,3,4,4,5,5-Hexafluoro-2-(2-methylbenzo[b]thiophen-3-yl)cyclopent-1-en-1-yl)-2-methyl-6-nitrobenzo[b]thiophene. PC-1 (89 mg) was added to 2.3 mL of glacial acetic acid and 0.2 mL of acetic anhydride in an ice bath. The flask was covered throughout the reaction to avoid exposure to light. Then 0.1 mL of fuming nitric acid was slowly added; meanwhile the solution was mixed vigorously and maintained at ∼5 °C. After 15 min the temperature was raised to 10 °C, and then the solution was allowed to react overnight. The reaction was quenched by the addition of 5 mL of water, at which point a white-yellow precipitate was observed. The solution was neutralized with (30 mL) concentrated aqueous NaOH. The crude reaction was extracted with ethyl acetate (2 × 25 mL), and the organic phase was washed with water, dried with Na_2SO_4, filtered, and evaporated in a Rotovap system. Purification was performed on a silica gel column with cyclohexane−ethyl acetate (98:2) as solvent, with a final product of 3-(3,3,4,4,5,5-hexafluoro-2-(2-methylbenzo[*b*]thiophen-3-yl)cyclopent-1-en-1-yl)-2-methyl-6-nitrobenzo[*b*]thiophene as a white-yellow solid (38.2 mg, 39%). Characterization was in accordance with reported information.[48]

PC-3 = 4-((3-(3,3,4,4,5,5-Hexafluoro-2-(2-methylbenzo[b]thiophen-3-yl)cyclopent-1-en-1-yl)-2-methylbenzo[b]thiophen-6-yl-)amino)-4-oxobutanoic Acid. A solution of PC-2 (24 mg) was prepared in 5 mL of methanol. $NiCl_2 \cdot 6H_2O$ (86.76 mg) was added under vigorous mixing until complete solubility of PC-2 was achieved. The solution was placed in an ice bath, and then $NaBH_4$ (43.5 mg) was slowly added, leading to the immediate formation of a black precipitate. The solution was allowed to react for 1 h at room temperature, quenched with 0.04 N HCl, filtered, and then evaporated in a Rotovap. The residue was extracted with dichloromethane (2 × 15 mL), and the organic phase was washed with water, dried with Na_2SO_4, filtered, and evaporated in a Rotovap. A pink oil (22.6 mg) was obtained and used as is in the synthesis of photochromic polymer.

Synthesis of Amphiphilic Photochromic Polymer. PMA (18.5 mg) was added to a dry glass flask. The recently prepared PC-3 (25.0 mg) was dissolved in anhydrous THF (5.5 mL) and added to the PMA in the flask. The added photochromic compound corresponded to an ∼10-fold excess over the anhydride monomers selected for conjugation with photochromic moieties. The aromatic nature of the amine as well as the relative bulk of the PC-3 reduces the yield of the coupling.[49] The flask was sonicated for 2 min and left to react at 50 °C with stirring. The solvent was reduced to approximately half, and the reaction was continued overnight. A solution of dodecylamine in THF (500 μL 25 g/L) was added and allowed to react at room temperature for 2 h. The dodecylamine coupling was assumed to be stoichiometric. The end point of the reaction can be observed as the solution changes from cloudy to a slightly yellow translucent solution. The preparation was dried and resuspended in anhydrous chloroform and purified from unreacted reagents using Sephadex LH-20 (GE Healthcare). The purification was followed by thin-layer chromatography. The obtained polymer was vacuum-dried (28.0 mg, 55%).

QD Phase Transfer. QD samples were precipitated from the toluene (solvent supplied by the manufacturer) and resuspended in anhydrous $CHCl_3$. An absorbance spectrum of the solution was taken so as to discern the concentration. A solution of the photochromic polymer was prepared in anhydrous $CHCl_3$. The total surface area of the QD solution was calculated. The *R* value is defined as the amount of monomer per nm^2 of QD surface. The solutions were mixed in a glass flask in proportion so as to achieve an *R* value of 100, previously determined to be the optimum coating condition.[50] The reaction was mixed at 40 °C for 30 min. Approximately half the solvent was evaporated. Mixing was continued for another hour. The rest of the solvent was evaporated slowly, and once the sample was dry, SBB pH 9 buffer in excess was added immediately. The samples were left overnight with mild stirring, then filtered with 0.2 μm inorganic syringe filters (Whatman, Anatop 10). An *R* of 100 was not achieved even in the presence of excess polymer. The estimates were closer to 40 monomers/nm^2 of QD surface, but even this number is unrealistically high inasmuch as it would correspond to a packing density of 2.5 $Å^2$/molecule.

psQD Purification. The purification of the psQDs was realized by filtration with 0.2 μm inorganic filters, after which the solutions were concentrated to the 1 μM range using Amicon 100 000 kDa cutoff filters (Millipore) and 50 mM sodium borate buffer (SBB), pH 9.0. Injections of 20 or 50 μL (depending on concentration) were applied to a Superdex 200 analytical column (GE Healthcare Life Science) in an HPLC system with three-wavelength UV−vis detection. Elution was with 50 mM SBB, pH 9, starting with a flow of 50 μL/min for 3 min and then

20 μL/min. The average run time was 70 min. Depending on the preparation, three or two peaks were observed. In the case of three peaks the initial two (30−35 min) corresponded to micelles of different sizes (290 $\pm$ 25 nm and 60 $\pm$ 9 nm group according to DLS) and the third to the QDs (45 min). With only two peaks, the initial peak corresponded to micelles and the second peak to the QDs. Depending on initial concentration and purity, a peak of monomeric polymer was sometimes observed at 60 min, usually as a low broad shoulder. In some cases a second injection was required to obtain the desired purity.

TEM. Samples of 0.1 μM concentration were prepared in 50 mM SBB buffer. They were stained with uranyl acetate, placed on a carbon grid, and imaged with a Philips 120 kV BioTwin microscope equipped with a 1024 $\times$ 1024 pixel GATAN CCD camera (Gatan, Inc.). The digital images were analyzed with the MATLAB (The MathWorks) toolbox DIPimage (Quantitative Imaging Group, Delft University of Technology). A total of 50−200 particles were measured to calculate diameter statistics.

DLS. Measurements were made with a Nano-ZS Zetasizer Nanoseries (Malvern Instruments) and a 90Plus particle size analyzer (Brookhaven Instruments). Solutions were filtered (when appropriate) with 0.22 μm inorganic syringe filters, and dilutions made with deionized water so as to achieve an optimal concentration of the sample. QD solutions could not be measured in the DLS systems because of the fluorescence of the sample.

Sample Irradiation. Samples were irradiated using an Hg arc lamp (SUV-DC, Lumatec, Deisenhofen, Germany) and filters (340 $\pm$ 10 and 545 $\pm$ 10 nm). Samples were placed in Hellma 10 $\times$ 2 mm microcuvettes, filled such that the entire sample was exposed to light, thereby eliminating mixing effects. The samples were kept dilute (<0.1 absorbance at 527 nm for all conversion rates) so as to avoid internal filter effects.

Spectroscopy. The levels of light utilized for monitoring the systems did not have an appreciable effect upon the photoconversion status of the samples.

Absorbance. Absorbance spectra (300−800 nm) were acquired on a Cary 100 UV−vis spectrophotometer (Varian) utilizing 100 μL microcuvettes with a 10 mm optical path. A solvent spectrum was utilized as a blank.

Fluorescence. Fluorescence spectra were acquired on a Cary Eclipse fluorescence spectrophotometer (Varian) utilizing Hellma 100 μL microcuvettes. Excitation and emission bandwidths were 5 nm, and the sample temperature was 20 °C. The usual excitation wavelength for QDs was 400 nm.

Lifetime Determinations. Fluorescence lifetime measurements were performed in a FluoroLog-TCSPC (Horiba Jobin Yvon). Excitation was carried out with a nanoLED N-320 source (Horiba Scientific), a time-to-amplitude converter (TAC) of 500 ns, pulse repetition frequencies of 500 kHz, and 50 000 counts for peak value. Emission counts were determined at QD fluorescence maximum. Mean lifetimes were calculated using three-component fitting with a Mathematica 7 program.[51]

Acknowledgment. We thank D. Arndt-Jovin, D. Yushchenko, M. Konrad, and W. Parak for valuable discussions, D. Riedel for the TEM images, and the Department of Physical Biochemistry, MPIbpcs, for the use of the TCSPC fluorimeter. This work was supported by the Max Planck Society (E.J.E., Partner Group grant; Toxic Protein Conformation project), Argentine agencies ANpCyT, CONICET, and UBA (E.J.E.), and Cluster of Excellence 171 of the DFG Centre for the Molecular Physiology of the Brain (DFG CMPB). S.A.D. received fellowships from ANpCyT (PICT 2006/01365), Kooperation International (BMBF: Project ARG 08/019), and Deutscher Akademischer Austauschdienst (Doctorate DAAD-Sandwich Scholarship #A/09/75106).

Supporting Information Available: Calculations of spectral constants and photoconversion extents; calculations of PC groups per polymer and per psQD; TEM image; fits to the photoconversion data. This material is available free of charge *via* the Internet at http://pubs.acs.org.

REFERENCES AND NOTES

1. Walling, M. A.; Novak, J. A.; Shepard, J. R. E. Quantum Dots for Live Cell and *in vivo* Imaging. *Int. J. Mol. Sci.* **2009,** *10*, 441–491.
2. Medintz, I. L.; Mattoussi, H. Quantum Dot-Based Resonance Energy Transfer and its Growing Application in Biology. *Phys. Chem. Chem. Phys.* **2009,** *11*, 17–45.
3. Clapp, A. R.; Medintz, I. L.; Mattoussi, H. Förster Resonance Energy Transfer Investigations Using Quantum-Dot Fluorophores. *ChemPhysChem* **2006,** *7*, 47–57.
4. Morgner, F.; Geissler, D.; Stufler, S.; Butlin, N. G.; Lohmannsroben, H. G.; Hildebrandt, N. A Quantum-Dot-Based Molecular Ruler for Multiplexed Optical Analysis. *Angew. Chem., Int. Ed.* **2010,** *49*, 7570–7574.
5. Roberti, M. J.; Giordano, L.; Jovin, T. M.; Jares-Erijman, E. A., FRET Imaging by k_t/k_f. *ChemPhysChem* 2011, *12*, DOI: 10.1002/cphc.201000925.
6. Giordano, L.; Jovin, T. M.; Irie, M.; Jares-Erijman, E. A. Diheteroarylethenes As Thermally Stable Photoswitchable Acceptors in Photochromic Fluorescence Resonance Energy Transfer (pcFRET). *J. Am. Chem. Soc.* **2002,** *124*, 7481–7489.
7. Jares-Erijman, E. A.; Jovin, T. M. FRET Imaging. *Nat. Biotechnol.* **2003,** *21*, 1387–1395.
8. Marriott, G.; Mao, S.; Sakata, T.; Ran, J.; Jackson, D. K.; Petchprayoon, C.; Gomez, T. J.; Warp, E.; Tulyathan, O.; Aaron, H. L.; *et al.* Optical Lock-In Detection Imaging Microscopy for Contrast-Enhanced Imaging in Living Cells. *Proc. Natl. Acad. Sci. U. S. A.* **2008,** *105*, 17789–17794.
9. Yan, Y.; Marriott, M. E.; Petchprayoon, C.; Marriott, G. Optical Switch Probes and Optical Lock-in Detection (OLID) Imaging Microscopy: High-Contrast Fluorescence Imaging within Living Systems. *Biochem. J.* **2011,** *433*, 411–422.
10. Reits, E. A. J.; Neefjes, J. J. From Fixed to FRAP: Measuring Protein Mobility and Activity in Living Cells. *Nat. Cell Biol.* **2001,** *3*, E145–E147.
11. Levitt, J. A.; Matthews, D. R.; Ameer-Beg, S. M.; Suhling, K. Fluorescence Lifetime and Polarization-Resolved Imaging in Cell Biology. *Curr. Opin. Biotechnol.* **2009,** *20*, 28–36.
12. Patterson, G.; Davidson, M.; Manley, S.; Lippincott-Schwartz, J. Superresolution Imaging Using Single-Molecule Localization. *Annu. Rev. Phys. Chem.* **2010,** *61*, 345–367.
13. Bates, M.; Huang, B.; Zhuang, X. Super-Resolution Microscopy by Nanoscale Localization of Photo-Switchable Fluorescent Probes. *Curr. Opin. Chem. Biol.* **2008,** *12*, 505–514.
14. Heilemann, M.; Dedecker, P.; Hofkens, J.; Sauer, M. Photoswitches: Key Molecules for Subdiffraction-Resolution Fluorescence Imaging and Molecular Quantification. *Laser Photonics Rev.* **2008,** *3*, 180–202.
15. Schermelleh, L.; Heintzmann, R.; Leonhardt, H. A Guide to Super-Resolution Fluorescence Microscopy. *J. Cell Biol.* **2010,** *180*, 165–175.
16. Dertinger, T.; Colyer, R.; Iyer, G.; Weiss, S.; Enderlein, J. Fast, Background-free, 3D Super-Resolution Optical Fluctuation Imaging (SOFI). *Proc. Natl. Acad. Sci. U. S. A.* **2009,** *106*, 22287–92.
17. Medintz, I. L.; Trammell, S. A.; Mattoussi, H.; Mauro, J. M. Reversible Modulation of Quantum Dot Photoluminescence Using a Protein- Bound Photochromic Fluorescence Resonance Energy Transfer Acceptor. *J. Am. Chem. Soc.* **2004,** *126*, 30–31.
18. Jares-Erijman, E. A.; Giordano, L.; Spagnuolo, C.; Lidke, K.; Jovin, T. M. Imaging Quantum Dots Switched On and Off by Photochromic Fluorescence Resonance Energy Transfer (pcFRET). *Mol. Cryst. Liq. Cryst.* **2005,** *430*, 257–265.
19. Erno, Z.; Yildiz, I.; Gorodetsky, B.; Raymo, F. M.; Branda, N. R. Optical Control of Quantum Dot Luminescence *via* Photoisomerization of a Surface-Coordinated, Cationic Dithienylethene. *Photochem. Photobiol. Sci.* **2010,** *9*, 249–253.
20. Piao, X.; Zou, Y.; Wu, J.; Li, C.; Yi, T. Multiresponsive Switchable Diarylethene and Its Application in Bioimaging. *Org. Lett.* **2009,** *11*, 3818–3821.
21. Yildiz, I.; Deniz, E.; Raymo, F. M. Fluorescence Modulation with Photochromic Switches in Nanostructured Constructs. *Chem. Soc. Rev.* **2009,** *38*, 1859–1867.
22. Tian, Z. Y.; Yu, J. B.; Wu, C. F.; Szymanski, C.; McNeill, J. Amplified Energy Transfer in Conjugated Polymer Nanoparticle Tags and Sensors. *Nanoscale* **2010,** *2*, 1999–2011.

23. Irie, M. Diarylethenes for Memories and Switches. *Chem. Rev.* **2000,** *100*, 1685–1716.
24. Hirose, T.; Matsuda, K.; Irie, M. Self-Assembly of Photochromic Diarylethenes with Amphiphilic Side Chains: Reversible Thermal and Photochemical Control. *J. Org. Chem.* **2006,** *71*, 7499–7508.
25. Tomasulo, M.; Deniz, E.; Sortino, S.; Raymo, F. M. Hydrophilic and Photochromic Switches Based on the Opening and Closing of [1,3]Oxazine Rings. *Photochem. Photobiol. Sci.* **2010,** *9*, 136–140.
26. Chen, J.; Zeng, F.; Wu, S.; Chen, Q.; Tong, Z. A Core−Shell Nanoparticle Approach to Photoreversible Fluorescence Modulation of a Hydrophobic Dye in AqueousMedia. *Chem.—Eur. J.* **2008,** *14*, 4851–4860.
27. Zhu, L.; Wu, W.; Zhu, M.-Q.; Han, J. J.; Hurst, H. K.; Li, A. D. Q. Reversibly Photoswitchable Dual-Color Fluorescent Nanoparticles As New Tools for Live-Cell Imaging. *J. Am. Chem. Soc.* **2007,** *129*, 3524–3526.
28. Chudakov, D. M.; Matz, M. V.; Lukyanov, S.; Lukyanov, K. Fluorescent Proteins and Their Applications in Imaging Living Cells and Tissues. *Physiol. Rev.* **2010,** *90*, 1103–1163.
29. Weng, J.; Ren, J. Luminescent Quantum Dots: A Very Attractive and Promising Tool in Biomedicine. *Curr. Med. Chem.* **2006,** *13*, 897–909.
30. Yu, W. W. Semiconductor Quantum Dots: Synthesis and Water-Solubilization for Biomedical Applications. *Expert Opin. Biol. Ther.* **2008,** *8*, 1571–1581.
31. Michalet, X.; Pinaud, F. F.; Bentolila, L. A.; Tsay, J. M.; Doose, S.; Li, J. J.; Sundaresan, G.; Wu, A. M.; Gambhir, S. S.; Weiss, S. Quantum Dots for Live Cells, in Vivo Imaging, and Diagnostics. *Science* **2005,** *307*, 538–544.
32. Hezinger, A. F. E.; Tessmar, J.; Goepferich, A. Polymer Coating of Quantum Dots−a Powerful Tool Toward Diagnostics and Sensorics. *Eur. J. Pharm. Biopharm.* **2008,** *68*, 138–152.
33. Pellegrino, T.; Manna, L.; Kudera, S.; Liedl, T.; Koktysh, D.; Rogach, A. L.; Keller, S.; Raedler, J.; Natile, G.; Parak, W. J. Hydrophobic Nanocrystals Coated with an Amphiphilic Polymer Shell: A General Route to Water Soluble Nanocrystals. *Nano Lett.* **2004,** *4*, 703–707.
34. Jańczewski, D.; Tomczak, N.; Khin, Y. W.; Han, M.-Y.; Vancso, G. J. Designer Multi-Functional Comb-Polymers for Surface Engineering of Quantum Dots on the Nanoscale. *Eur. Polym. J.* **2009,** *45*, 3–9.
35. Kawai, T.; Kunitake, T.; Irie, M. Novel Photochromic Conducting Polymer Having Diarylethene Derivative in the Main Chain. *Chem. Lett.* **1999,** 905–906.
36. Wigglesworth, T. J.; Myles, A. J.; Branda, N. R. High-Content Photochromic Polymers Based on Dithienylethenes. *Eur. J. Org. Chem.* **2005,** 1233–1238.
37. Ercole, F.; Davis, T. P.; Evans, R. A. Photo-Responsive Systems and Biomaterials: Photochromic Polymers, Light-Triggered Self-Assembly, Surface Modification, Fluorescence Modulation and Beyond. *Polym. Chem.* **2010,** *1*, 37–54.
38. Fernandez-Argelles, M. T.; Yakovlev, A.; Sperling, R. A.; Luccardini, C.; Gaillard, S.; Medel, A. S.; Mallet, J.-M.; Brochon, J.-C.; Feltz, A.; Oheim, M.; *et al*. Synthesis and Characterization of Polymer-Coated Quantum Dots with Integrated Acceptor Dyes as FRET-Based Nanoprobes. *Nano Lett.* **2007,** *7*, 2613–2617.
39. Lin, C.-A. J.; Sperling, R. A.; Li, J. K.; Yang, T.-Y.; Li, P.-Y.; Zanella, M.; Chang, W. H.; Parak, W. J. Design of an Amphiphilic Polymer for Nanoparticle Coating and Functionalization. *Small* **2008,** *4*, 334–341.
40. Giordano, L.; Vermeij, R. J.; Jares-Erijman, E. A. Synthesis of Indole-Containing Diheteroarylethenes. New Probes for Photochromic FRET (pcFRET). *ARKIVOC* **2005,** 268–281.
41. Derfus, A. M.; Chan, W. C. W.; Bhatia, S. N. Probing the Cytotoxicity of Semiconductor Quantum Dots. *Nano Lett.* **2004,** *4*, 11–18.
42. Zhelev, Z.; Jose, R.; Nagase, T.; Ohba, H.; Bakalova, R.; Ishikawa, M.; Baba, Y. Enhancement of the Photoluminescence of CdSe Quantum Dots During Long-Term UV-Irradiation: Privilege or Fault in Life Science Research? *J. Photochem. Photobiol. B: Biol.* **2004,** *75*, 99–105.
43. Grecco, H. E.; Lidke, K. A.; Heintzmann, R.; Lidke, D. S.; Spagnuolo, C.; Martinez, O. E.; Jares-Erijman, E. A.; Jovin, T. M. Ensemble and Single Particle Photophysical Properties (Two-Photon Excitation, Anisotropy, FRET, Lifetime, Spectral Conversion) of Commercial Quantum Dots in Solution and in Live Cells. *Microsci. Res. Tech.* **2004,** *65*, 169–179.
44. Niebling, T.; Zhang, F.; Ali, Z.; Parak, W. J.; Hemibrodt, W. Excitation Dynamics in Polymer-Coated Semiconductor Quantum Dots with Integrated Dye Molecules: The Role of Reabsorption. *J. Appl. Phys.* **2009,** *106*, 104701–104701-6.
45. Wohlfarth, C.; Wohlfahrt, B., Condensed Matter Optical Constants. Refractive Indices of Pure Liquids and Binary Liquid Mixtures (Supplement to III/38). In *The Landolt-Börnstein Database*; Springer-Verlag: Berlin, 2008; Vol. 47.
46. Schreiber, F. Structure and Growth of Self-assembling Monolayers. *Prog. Surf. Sci.* **2000,** *65*, 151–256.
47. Hanazawa, M.; Sumiya, R.; Horikawa, Y.; Irie, M. Thermally Irreversible Photochromic Systems−Reversible Photocyclization of 1,2-Bis(2-methylbenzo[*b*]thiophen-3-yl)perfluorocycloalkene Derivatives. *J. Chem. Soc., Chem. Commun* **1992,** 206–207.
48. Kim, E.; Kim, M.; Kim, K. Diarylethenes with Intramolecular Donor-Acceptor Structures for Photo-induced Electrochemical Change. *Tetrahedron* **2006,** *62*, 6814–6821.
49. Hu, G. H.; Lindt, J. T. Amidification of Poly(styrene-co-maleic anhydride) with Amines in Tetrahydrofuran Solution: A Kinetic Study. *Polym. Bull.* **1992,** *29*, 357–363.
50. Sperling, R. A.; Pellegrino, T.; Li, J. K.; Chang, W. H.; Parak, W. J. Electrophoretic Separation of Nanoparticles with a Discrete Number of Functional Groups. *Adv. Funct. Mater.* **2006,** *16*, 943–948.
51. Celej, M. S.; Jares-Erijman, E. A.; Jovin, T. M. Fluorescent N-arylaminonaphthalene Sulfonate Probes for Amyloid Aggregation of α-Synuclein. *Biophys. J.* **2008,** *94*, 4867–4879.